Aalborg Universitet

AALBORG UNIVERSITY
DENMARK

3D Channel Model Emulation in a MIMO OTA Setup

Fan, Wei; Kyösti, Pekka; Sun, Fan; Nielsen, Jesper Ødum; Carreño, Xavier; Pedersen, Gert Frølund; Knudsen, Mikael

Published in:
Vehicular Technology Conference (VTC Fall), 2013 IEEE 78th

DOI (link to publication from Publisher):
10.1109/VTCFall.2013.6692020

Publication date:
2013

Document Version
Early version, also known as pre-print

Link to publication from Aalborg University

Citation for published version (APA):
Fan, W., Kyösti, P., Sun, F., Nielsen, J. Ø., Carreño, X., Pedersen, G. F., & Knudsen, M. (2013). 3D Channel Model Emulation in a MIMO OTA Setup. In *Vehicular Technology Conference (VTC Fall), 2013 IEEE 78th* (pp. 1-5). IEEE. I E E E V T S Vehicular Technology Conference. Proceedings
https://doi.org/10.1109/VTCFall.2013.6692020

General rights
Copyright and moral rights for the publications made accessible in the public portal are retained by the authors and/or other copyright owners and it is a condition of accessing publications that users recognise and abide by the legal requirements associated with these rights.

- Users may download and print one copy of any publication from the public portal for the purpose of private study or research.
- You may not further distribute the material or use it for any profit-making activity or commercial gain
- You may freely distribute the URL identifying the publication in the public portal -

Take down policy
If you believe that this document breaches copyright please contact us at vbn@aub.aau.dk providing details, and we will remove access to the work immediately and investigate your claim.

Downloaded from vbn.aau.dk on: July 01, 2022

3D Channel Model Emulation in a MIMO OTA Setup

Wei Fan[1], Pekka Kyösti [2], Fan Sun[1], Jesper Ø. Nielsen[1], Xavier Carreño[3], Gert F. Pedersen[1] and Mikael B. Knudsen[3]
[1]Department of Electronic Systems, Faculty of Engineering and Science, Aalborg University, Denmark
Email: wfa@es.aau.dk
[2]Anite Telecoms Oy, Finland
[3]Intel Mobile Communications, Aalborg, Denmark

***Abstract*—This paper presents a new channel reconstruction technique for 3D geometry-based channels in a multi-probe based MIMO OTA setup. The proposed method provides a general channel reconstruction framework for any spherical power spectrum. The channel reconstruction is formed as convex optimization problems, which give global optimal reconstruction accuracy and allow for a relatively low computational complexity.**

I. Introduction

As a solution to evaluate multiple input multiple output (MIMO) device performance in realistic conditions in the lab, MIMO over the air (OTA) testing has attracted huge interest from both industry and academia [1], [2]. Standardization work for the development of the MIMO OTA test methods is ongoing in CTIA, 3GPP and COST IC1004 [1]. One promising candidate is the multi-probe based anechoic chamber method. Compared to field testing, the anechoic chamber based MIMO OTA testing provides repeatable and controllable testing environments, so the major challenge is to emulate a realistic environment which can accurately reflect the real wireless propagation environment.

Most of the standard channel models in the literature are two-dimensional (2D). That is, the channel models are defined only on the azimuth plane and no spread over elevation dimension is assumed [3], [6]. These models are valid in the scenarios where the elevation spread of the incoming power spectrum is concentrated on a very narrow elevation-angle region at the elevation angle $\theta = 0^o$ in typical spherical coordinates in the propagation literature. 2D standard channel models are used in the MIMO OTA testing so far [1]. Several contributions in the literature have addressed techniques to emulate the 2D standard channel models in a multi-probe setup [2], [5]. However, the 2D channel model assumption is not generally valid. Measurements have demonstrated that elevation spread can not be ignored in many propagation environments. Various distributions have been proposed for power azimuth spectrum (PAS) and power elevation spectrum (PES) of the incoming power spectrum [6], [7], [8], [9].

In order to evaluate MIMO terminals in realistic environments in the lab, it would be desirable that the 3D radio channels can be accurately reproduced in a multi-probe MIMO OTA setup. Very few contributions have addressed this issue. In [10], it was briefly mentioned that 32 symmetrically placed OTA probes in a 3D setup were used to emulate 3D channel models, but no algorithm description is given. In [11], the 3D channel reconstruction technique is briefly described. The test volume where the device under test (DUT) is located is sampled by selecting locations on three orthogonal segments of line inside the test volume.

In the current paper, a novel 3D channel model reconstruction technique in a MIMO OTA setup is proposed, where the test volume is sampled by locations on the surface of an ellipsoid shaped test volume. The 3D channel reconstruction technique has also been implemented in a commercial channel emulator EB Propsim F8, where the Laplacian distribution is defined for PAS and PES. For the proposed reconstruction technique, there is no limitation on the spherical power spectrum shape. The main work of this paper is to extend the 2D prefaded signal synthesis (PFS) technique [2] for 3D channel models. The focus is on reproducing the spatial structure of the 3D channel with a limited number of probes in a 3D configuration. Note that the notation channel reconstruction is interchangable with channel emulation in this paper. The contributions of this work are:

- We first form the 3D channel reconstruction problem via two objectives: the sum reconstruction error minimization and the maximal reconstruction error minimization. The first one minimizes the summation over the total reconstruction errors while the second one avoids potential high peaks of reconstruction error. Both problems are convex optimization problems when the OTA probe positions are fixed, which can be solved efficiently [12]. Employing the convex optimization framework into the channel reconstruction can greatly reduce the computational complexity.
- Selecting points on the surface of the test volume to form the samples, offers better reconstruction accuracy than that obtained by using points on three orthogonal lines inside test volume, as reported in [11].
- The proposed reconstruction method provides a general reconstruction framework for any spherical power spectrum.

II. Method

A. Reconstruction technique for 2D channel models

Several papers have discussed OTA testing setups for MIMO devices with emphasis on channel modeling, where the goal

is to accurately reproduce realistic 2D channels in the test area inside the chamber with a limited number of OTA probes [2], [14]. The prefaded signals synthesis (PFS) technique, as detailed in [2], is able to create radio propagation environments for OTA testing and has been verified in practical MIMO OTA systems [13]. The modeling of radio channel parameters such as delay, Doppler, channel polarization and transmitter (Tx) side spatial characteristics is detailed in [2] and can be easily modeled. Thus, the focus is on reproducing receiver (Rx) side spatial aspects of the channel, which is critical as we extend Single Input Single Output (SISO) OTA to MIMO OTA testing.

In [10], a 3D geometry-based radio channel model based on [6] was presented, where the elevation dimension is introduced to extend the standard 2D geometry-based channel to the full 3D model. As explained in [2], the PFS technique works the same for vertically and horizontally polarized power spectrum. This rule applies to the 3D case as well and the polarization is omitted for the sake of simplicity.

B. Model of 3D spherical power spectrum

The spherical power spectrum needs to be modeled as a function of both elevation angle (θ) and azimuth angle (ϕ). The spherical power spectrum is often modeled separately in azimuth and elevation [9], [11]:

$$P(\theta, \phi) = P(\theta)P(\phi) \tag{1}$$

where $P(\theta)$, $P(\phi)$ are the PES and PAS, respectively. The spherical power spectrum $P(\theta, \phi)$ needs to satisfy the following condition:

$$\oint P(\Omega)d\Omega = \int_{-\pi}^{\pi} \int_{-\pi/2}^{\pi/2} P(\theta, \phi) \cos\theta d\theta d\phi = 1 \tag{2}$$

where Ω is the solid angle.

The spherical power spectrum shape has been investigated in the literature. Several models have been proposed for the PAS and PES based on measurements. Wrapped Gaussian, uniform, truncated Laplacian and von Mises distribution have been proposed for the PAS distribution, while wrapped Gaussian, truncated Laplacian are often used for the PES distribution [7], [8], [9]. Note that this work is not restricted to any model, and spherical power spectrum based on measurements can also be reconstructed as well. In this paper, the PAS is defined with an interval of $[\phi_0 - \pi, \phi_0 + \pi]$ of size 2π centered at azimuth angel of arrival (AoA) ϕ_0, while the PES is with an interval of $[\theta_0 - \frac{\pi}{2}, \theta_0 + \frac{\pi}{2}]$ of size π centered at elevation angle of arrival (EoA) θ_0.

The example distributions are described by the following expressions:

a) Uniform power distribution:

$$P(\phi) = \frac{1}{2\pi}, \quad \phi \in [-\pi, \pi] \tag{3}$$

b) Truncated Gaussian power distribution:

$$P(\epsilon) = \frac{Q_G}{\sqrt{2\pi}\sigma} \exp\left[-\frac{(\epsilon - \epsilon_0)^2}{2\sigma^2}\right], \tag{4}$$

c) Truncated Laplacian power distribution:

$$P(\epsilon) = \frac{Q_L}{\sqrt{2\pi}\sigma} \exp\left[-\frac{\sqrt{2}|\epsilon - \epsilon_0|}{\sigma}\right], \tag{5}$$

d) Von Mises distribution power distribution :

$$P(\theta) = \frac{\exp[a\cos(\theta - \theta_0)]}{2\pi I_0(a)}, \tag{6}$$

where $P(\epsilon)$ denotes either the PAS distribution $P(\phi)$ or the PES distribution $P(\theta)$. Q_G and Q_L are scaling constants ensuring that (2) is fulfilled. σ is the standard deviation. a controls the angle spread of the von Mises distribution.

C. Criteria to model 3D channel spatial characteristics

The spatial correlation is a statistical measure of the similarity of the received signals and it is selected as a figure of merit (FoM) to model 3D channel spatial characteristics, similar to the 2D case [2]. For the 2D channel reconstruction, the spatial correlation between two antenna elements u and v is calculated based on the assumption that two antenna elements exhibit the same omnidirectional radiation pattern and the phase difference is determined by the wavelength and relative positions of two antenna elements. This is due to the fact that the DUT antenna pattern is typically not known beforehand and if some antenna patterns are otherwise embedded to the channel model for channel reconstruction, the channel model itself will assume some DUT antennas. Similar to [2], isotropic antenna patterns are assumed for the 3D channel reconstruction in this paper.

The spatial correlation can be determined according to [4], for a single polarization, as:

$$\rho_a = \frac{\oint G_u(\Omega) G_v^\star(\Omega) P(\Omega) d\Omega}{\sqrt{\oint |G_u(\Omega)|^2 P(\Omega) d\Omega} \sqrt{\oint |G_v(\Omega)|^2 P(\Omega) d\Omega}}, \tag{7}$$

where $()^\star$ denotes complex conjugate operation, G_u and G_v are the complex radiation patterns of antennas u and v, respectively, with a common phase center.

From (2) and the assumption about the isotropic antenna pattern, we can rewrite equation (7) as:

$$\rho = \oint \exp(jk(\overline{r}_u - \overline{r}_v) \cdot \overline{\Omega}) P(\Omega) d\Omega, \tag{8}$$

where $\overline{r}_u$ and $\overline{r}_v$ are vectors containing the position information of antenna u and v, respectively. $\overline{\Omega}$ is an unit vector denoting space angle Ω. $(\cdot)$ is the dot product operator. k is the wave number.

D. 3D channel reconstruction

In the MIMO OTA setup, the goal is to obtain OTA probe power weights so as to minimize the deviation between the theoretical spatial correlation from a target continuous spherical power spectrum, and the emulated correlation from a discrete spherical power spectrum characterized by power weights of the probes.

Similar to (8), the emulated spatial correlation can be calculated based on the discrete spherical power spectrum characterized by M probes as:

$$\hat{\rho} = \sum_{m=1}^{M} w_m \exp(jk(\overline{r}_u - \overline{r}_v) \cdot \overline{\Phi}_m), \tag{9}$$

where w_m is the power weight for the mth probe. $\overline{\Phi}_m$ is an unit position vector of the mth probe. M is the number of probes. We further assume there are N location pairs for antenna u and v (sample points) on the test volume for reconstruction purpose. Therefore, we have $\hat{\rho}_i$, $1 \leq i \leq N$. We will discuss two different objective functions as follows:

1) Minimizing sum reconstruction errors (Min-Sum): The objective is to minimize the summation over the total reconstruction errors across all the location pairs:

$$\begin{aligned} \min_{\boldsymbol{w}} \quad & \|\hat{\boldsymbol{\rho}}(\boldsymbol{w}) - \boldsymbol{\rho}\|_2^2 \\ s.t. \quad & 0 \leq w_m \leq 1, \ \forall m \in [1, M] \end{aligned} \tag{10}$$

where $\boldsymbol{w} = [w_1, ..., w_M]^T$ is a power weighting vector to be optimized. $\hat{\boldsymbol{\rho}}$ and $\boldsymbol{\rho}$ are the reconstructed spatial correlation and target spatial correlation vectors with each element corresponding to the spatial correlation between two isotropic antennas at a certain location pair inside the test volume. The optimal vector of OTA antenna power weights $\boldsymbol{w}$ can be obtained by solving the objective function (10), which is a quadratic programming problem with linear constraints when the probe positions are fixed. Therefore, we can easily solve the problem in (10) via a popular convex problem solver CVX in [12].

2) Minimizing maximal reconstruction error (Min-Max) : An alternative objective function is:

$$\begin{aligned} &\min_{\boldsymbol{w}} \ \max_i |\hat{\rho}_i - \rho_i| \\ &s.t. \ 0 \leq w_m \leq 1, \ \forall m \in [1, M]. \end{aligned} \tag{11}$$

Through this objective function, we minimize the largest reconstruction error $\max_i |\hat{\rho}_i - \rho_i|$ and avoid potential high peaks in the reconstruction errors. However, this surely leads to a loss in terms of the total reconstruction errors $\|\hat{\boldsymbol{\rho}}(\boldsymbol{w}) - \boldsymbol{\rho}\|_2^2$, which will be demonstrated via simulation results later. Eq. (11) can be equivalently transformed into

$$\begin{aligned} &\min_{\boldsymbol{w}} \ t \\ &s.t. \ |\hat{\rho}_i - \rho_i| \leq t, \ \forall i \in [1, N], \ t \geq 0 \\ &\quad 0 \leq w_m \leq 1, \ \forall m \in [1, M]. \end{aligned} \tag{12}$$

Thus, after the equivalent transformation, (12) is again a convex problem, which can be handled efficiently via CVX in [12].

3) Sampling the test volume: In [10] and [11], it is mentioned that the sphere shaped test volume in the center of the 3D OTA setup is sampled by selecting locations u and v from three orthogonal segments of line inside the sphere, as shown in Figure 1 (red points on three orthogonal lines). This way of selecting sample points within the test volume will give optimal results on the three axes. However, it might not present optimal reconstruction results for sample points within whole the test volume and reconstruction accuracy might be critically bad at certain locations. In a practical MIMO OTA measurement, antennas on the DUT may be arbitrarily placed inside the test volume.

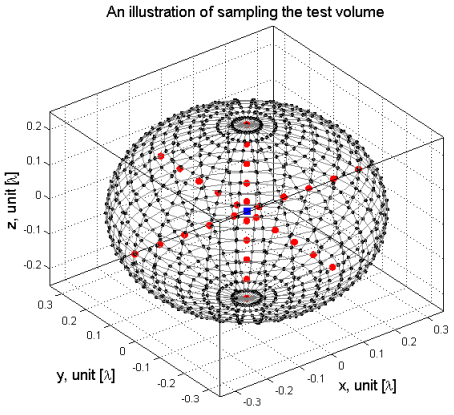

Figure 1. An illustration of different ways to sample the test volume. Blue mark denotes the test volume center. One way is to select locations u and v from three orthogonal axes (red marks), as shown in [10], [11]. Another way is to select locations u and v on the surface of test volume which are directly opposite each other (black marks).

In this paper, the oblate ellipsoid shaped test volume is proposed instead of the sphere, as the number of OTA probes in the azimuth plane is likely different from that in the elevation plane. The test volume is sampled by selecting locations on the surface of the ellipsoid. Positions for u and v ($\overline{r}_u$ and $\overline{r}_v$) are on the surface of the test volume and directly opposite to each other w.r.t the test volume center. Sample points are obtained by sweeping the location pairs over the whole surface of the ellipsoid, as illustrated in Figure 1.

III. Simulation Results

A. Comparison of reconstruction accuracy for different algorithms

The 3D reconstruction technique is implemented in the commercial channel emulator EB Propsim F8 where the PAS and PES are defined for the Laplacian distribution. In this section, the proposed algorithms are compared with the emulated results from the EB channel emulator.

Three test scenarios are considered, as detailed in Table I. Three different probe configurations and target spherical power spectrum are assessed. For each target spherical power spectrum, AoA and azimuth spread of arrival (ASA) are defined for the Laplacian shaped PAS; while EoA and elevation spread of arrival (ESA) are specified for the Laplacian shaped PES. The DUT size should be smaller than the test volume to ensure that the target propagation environment is accurately reproduced around the DUT. The test volume of case A is illustrated in Figure 1. Test volume in case C is larger than that in case A due to the fact that more probes are used in case C.

Three probe setups are shown in Figure 2(a), Figure 2(b) and Figure 2(c), respectively. Probe angular location details

Table I
TEST CASES CONSIDERED FOR ALGORITHM COMPARISON

Test Case	Probe Setup	Target Spherical Power Spectrum		
		PAS shape	PES shape	Test volume
A	A	AoA = 0^o ASA = 35^o	EoA = 0^o ESA = 10^o	Major axis: 0.7λ Minor axis: 0.5λ
B	B	AoA = 0^0 ASA = 35^o	EoA = 15^o ESA = 10^o	Major axis: 1.8λ Minor axis: 0.9λ
C	C	AoA = 0^o ASA = 35^o	EoA = 0^o ESA = 10^o	Major axis: 2λ Minor axis: 0.6λ

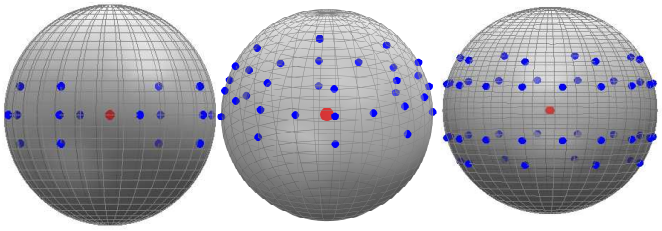

(a) Probe setup A (b) Probe setup B (c) Probe setup C

Figure 2. Three probe configurations used for algorithm comparison. Red mark denotes the center of 3D sphere and blue marks denote the position of probes on the sphere, as detailed in Table II.

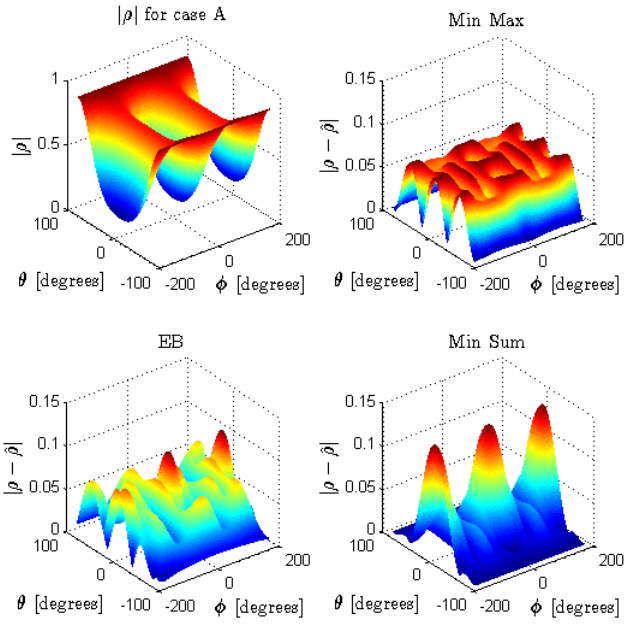

Figure 3. Target spatial correlation $|\rho|$ between antenna u and v on the surface of the test volume for case A and associated reconstruction results $|\rho - \hat{\rho}|$ with different algorithms.

are shown in Table II. The probes are placed on a sphere. and the elevation angle θ and the azimuth angle ϕ are specified for each probe. The probes are organized on several elevation rings. θ_i denotes the elevation angle for all the probes on ith elevation ring. ϕ_{ij} is the azimuth angle of the jth probe on the ith elevation ring.

The target spatial correlation $|\rho|$ for the test case A and reconstruction results with different algorithms are shown in Figure 3. The spatial correlation between the antennas on the surface of the test volume varies with locations of antennas. The reconstruction accuracy depends on the probe setup, the target channel and the number of probes. Statistics of the reconstruction results for all cases with different algorithms are summarized in Table III. Generally, the Min-Sum algorithm presents the best performance for all scenarios in terms of rms error, while the Min-Max algorithm offers the smallest maximal error for all cases, as explained and consistent with the algorithm description in Section II-D. The Min-Max and Min-Sum algorithms give comparable reconstruction accuracies for the test case C.

The algorithm implemented in the EB channel emulator generally offers good results for the spatial correlation over three orthogonal axes probably due to the fact that the sample points for optimization are on the three axes [11], as shown in Figure 4. However, as explained before, this way of sampling the test volume might not give globally optimal reconstruction results for the whole test volume and the reconstruction accuracy might be critical at certain locations. As shown in Table III, the EB algorithm results slightly worse rms error in all the three test cases compared to the Min-Sum algorithm and clearly worse maximum error compared to the Min-Max algorithm.

Table II
PROBE ANGULAR LOCATION DETAILS

Case	Detail		
	Total	Setup	Angular location
A	16	3 elevation rings	$\theta_1 = -15^o\ \phi_{1j} = -180^o + j \cdot 90^o, j \in [1, \ldots, 4]$
			$\theta_2 = 0^o\ \phi_{2j} = -180^o + j \cdot 45^o, j \in [1, \ldots, 8]$
			$\theta_3 = 15^o\ \phi_{3j} = -180^o + j \cdot 90^o, j \in [1, \ldots, 4]$
B	32	3 elevation rings	$\theta_1 = 0^o\ \phi_{1j} = -180^o + j \cdot 45^o, j \in [1, \ldots, 8]$
			$\theta_2 = 15^o\ \phi_{2j} = -180^o + j \cdot 22.5^o, j \in [1, \ldots, 16]$
			$\theta_3 = 30^o\ \phi_{3j} = -180^o + j \cdot 45^o, j \in [1, \ldots, 8]$
C	48	4 elevation rings	$\theta_1 = -30^o\ \phi_{1j} = -180^o + j \cdot 45^o, j \in [1, \ldots, 8]$
			$\theta_2 = -15^o\ \phi_{2j} = -180^o + j \cdot 22.5^o, j \in [1, \ldots, 16]$
			$\theta_3 = 15^o\ \phi_{3j} = -180^o + j \cdot 22.5^o, j \in [1, \ldots, 16]$
			$\theta_4 = 30^o\ \phi_{4j} = -180^o + j \cdot 45^o, j \in [1, \ldots, 8]$

Table III
STATISTICS OF THE RECONSTRUCTION RESULTS $|\rho - \hat{\rho}|$ WITH DIFFERENT ALGORITHMS FOR ALL SCENARIOS

Case	EB		Min-Sum		Min-Max	
	rms	max	rms	max	rms	max
A	0.0458	0.1030	0.0402	0.1315	0.0497	0.0672
B	0.0722	0.1933	0.0470	0.1823	0.0580	0.0924
C	0.1581	0.3558	0.1295	0.2665	0.1295	0.2665

B. Channel reconstruction for different spherical power spectra

The proposed algorithm is a general reconstruction technique for any spherical power spectrum. The spherical power spectrum discussed in Section II-B and the measurement based practical shape can be emulated as well.

A target channel detailed in Table IV is used to demonstrate the idea. The target spatial correlation $|\rho|$ between antenna u and v on the surface of the test volume for the case D and the associated reconstruction results $|\rho - \hat{\rho}|$ is shown in

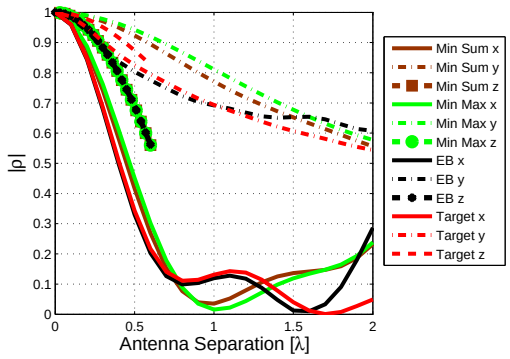

Figure 4. Target spatial correlation $|\rho|$ between antenna u and v on three orthogonal axes and emulated spatial correlation $|\hat{\rho}|$ with different algorithms for case C.

Table IV
TEST CASES CONSIDERED FOR ALGORITHM DEMONSTRATION

Test Case	Probe Setup	Target Spherical Power Spectrum		
		PAS shape	PES shape	Test volume
D	A	Uniform PAS	EoA = 0^o ESA = 10^o	Major axis: 0.7λ Minor axis: 0.5λ

Figure 5. The target spatial correlation $|\rho|$ is constant over azimuth angles due to the uniform PAS model assumption. reconstruction error $|\rho - \hat{\rho}|$ is below 0.03 for the test case D. Figure 6 shows the target spatial correlation $|\rho|$ and emulated spatial correlation $|\hat{\rho}|$ on three orthogonal axes. Therefore, the spatial correlation values on x and y axes coincide due to the uniform PAS model assumption. In the probe setup A, 16 probes offers good reconstruction accuracy for the test case D.

IV. CONCLUSION

This paper presents a channel reconstruction technique for 3D geometry-based channel models in a multi-probe based setup. The proposed methods, which provides a general reconstruction framework for any spherical power spectrum, offers globally optimal reconstruction accuracy and allows for a low computational complexity. In future work, we will further investigate the impact of number of probes, probe configurations, and channel models on the test volume size.

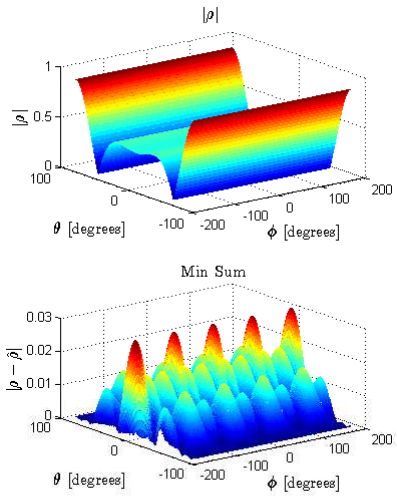

Figure 5. Target spatial correlation $|\rho|$ between antenna u and v on the surface of the test volume for case D and associated reconstruction results $|\rho - \hat{\rho}|$ with Min-Sum algorithm.

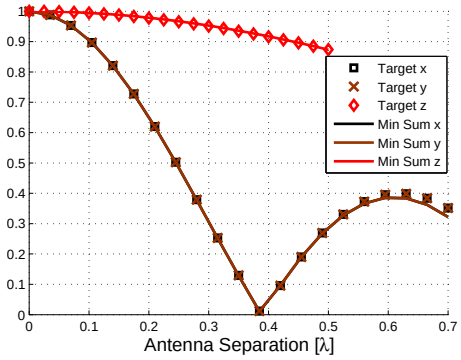

Figure 6. Target spatial correlation $|\rho|$ between antenna u and v on three orthogonal axes and emulated spatial correlation $|\hat{\rho}|$ for case D.

REFERENCES

[1] David A. Sanchez-Hernandez, Moray Rumney, Ryan J. Pirkl, and Markus Herrmann Landmann. MIMO Over-The-Air Research, Development, and Testing. Hindawi Journal of Antenna and Propagation. 9 May 2012.

[2] Pekka Kyösti, Tommi Jamsa, and Jukka-Pekka Nuutinen, Channel Modelling for Multiprobe Over-the-Air MIMO Testing, International Journal of Antennas and Propagation, vol. 2012, Article ID 615954, 11 pages, 2012. doi:10.1155/2012/615954.

[3] D. S. Baum, et al, "An interim channel model for beyond-3G systems: extending the 3GPP spatial channel model (SCM)," in Proceedings of the 61st IEEE Vehicular Technology Conference (VTC '05), vol. 5, pp. 3132– 3136, Stockholm, Sweden, May-June 2005.

[4] R. Vaughan and J. B. Andersen, Channels, Propagation and Antennas forMobile Communications, IET, London, UK, 2003.

[5] M. A. Mow, B. Niu, R. W. Schlub, R. Caballero, inventor; 2011 Nov. 3. TOOLS FOR DESIGN AND ANALYSIS OF OVER-THE-AIR TEST SYSTEMS WITH CHANNEL MODEL EMULATION CAPABILITIES. United States patent US 2011/0270567.

[6] 1ST-WINNER II Deliverable J.J.2 v.l .2. "WINNER II Channel Models," 1ST-WINNER II. Tech. Rep., 2007.

[7] K. Kalliola, H. Laitinen, P. Vainikainen, M. Toeltsch, J. Laurila, E. Bonek, "3-D Double-Directional Radio Channel Characterisation for Urban Macrocellular Applications," IEEE Transactions on Antennas and Propagation 2003.

[8] T. Taga, "Analysis for mean effective gain of mobile antennas in land mobile radio environments," IEEE Trans. Veh. Technol., vol. 39, pp. 117–131, May 1990.

[9] M.B. Knudsen, and G.F. Pedersen, "Spherical outdoor to indoor power spectrum model at the mobile terminal," IEEE Journal on Selected Areas in Communications, Vol. 20, No. 6, 1156-1169, 2002.

[10] L. Hentila, P. Kyösti, and J. Meinila, "Elevation Extension for a geometry based radio channel model and its influence on MIMO antenna correlation and gain imbalance," in Proc. of EuCAP 2011, Rome, Italy, April 2011.

[11] P. Kyösti and A. Khatun, "Probe Configurations for 3D MIMO Over-the-Air Testing," in Proc. of EuCAP 2013, Gothenburg, Sweden, April, 2013. (Accepted)

[12] S. Boyd and L. Vandenberghe, Convex Optimization. Cambridge, U.K.: Cambridge Univ. Press, 2004.

[13] Fan, Wei, et al. "Channel Verification Results for the SCME models in a Multi-Probe Based MIMO OTA Setup." Vehicular Technology Conference (VTC Fall), 2013 IEEE. (submitted)

[14] J. D. Reed, inventor; 2011 Dec. 8. EMULATION AND CONTROLLED TESTING OF MIMO OTA CHANNELS. United States patent US 2011/0299570.